2023 IEEE/ASME International Conference on Advanced Intelligent Mechatronics (AIM)
June 28-30, 2023. Seattle, Washington, USA

Disturbance-Observer-Based Admittance Control and Its Application to Safe Contact Regulation*

Kosuke Shikata[1] and Seiichiro Katsura[1]

Abstract— **Robust force control systems guarantee robustness to disturbance, including external force. Few previous studies, however, clarify transitions between contact and non-contact. This paper considers an admittance control with the desired relation between force and velocity to achieve safety transitions. Also, the proposed admittance control keeps robust by disturbance observer (DOB). The DOB-based admittance control intrinsically contains robust force control, and a controller during non-contact and one during contact differ only in damping parameter settings. It allows simple contact regulation on transitions. Experiments adopt and validate the proposed method for workspace control of two-degree-of-freedom (2-DOF) manipulators. This paper indicates that the control-based approach, as well as the mechanism-based approach, is one of the effective strategies in human-robot coexisting situations.**

I. Introduction

Force control [1]–[19] is one of the key technologies to realize robotic systems that coexist with humans. In coexisting situations, the systems face environmental changes. Since position control requires reference trajectory or target position as inputs, it can lack responsiveness to the changes in case of the inability to update them. Force control obeys the external force and enables the systems to work safely in coexisting areas or run smoothly like humans. Robust force control [1]–[3] is an explicit force control that focuses on improving robustness to variations between the system and the contact environment using disturbance observer (DOB) [2]. Despite the performance during contact, the current robust force control does not clearly emphasize transitions between contact and non-contact. The control system becomes the open-loop system during free motion and produces accelerated motion [3], which may influence contact stability.

Viscoelasticity provides stability to the contact and may solve the transition problems. There are mainly two ways to introduce viscoelasticity into a force control system; one is to insert actual viscoelastic elements, and the other is to provide viscous and elastic characteristics by designing controllers. As the mechanical approaches, force controllers for a series elastic/viscoelastic actuator (SEA) [4]–[6] and an elastic arm [7], [8] have been proposed. Force control system with mechanical viscoelasticity enables contact while suppressing impulsive force response. However, the mechanical approaches have a directionality effect that depends on the mechanical structure. The latter control approaches should also attract interest. Compliant control is a general term for control systems that provide viscoelasticity in response to applied forces, which is broadly divided into impedance [9], [10] and admittance controls [11]–[16].

This paper presents a force control system and the transition. During free motion in the coexisting situations, controllers have difficulty creating trajectory references since they do not know the exact distance to the target object or surface. Under such a constraint, the proposed control must realize a fast approach, impulsive force reduction, and force tracking performance. This paper proposes a novel admittance control based on disturbance suppression by DOB. The structure of the admittance controller has differences from the conventional one based on inner position [11]–[13] or velocity [14]–[16] loops and cancels the modeling error between actuators and the admittance model. The proposed controller can be considered a comprehensive type of robust force control. Furthermore, this paper regards the transitions as ones between three phases; approach, contact, and constrained phases. Unlike the impedance control [9], the admittance control-based method requires no trajectory references and is resistant to environmental changes. Because the proposed admittance control encompasses the robust force control, it does not require significant switching of control systems [17], [18]. Gain-switching occurs at the transition from the contact to the constrained phases, not from the approach to contact phases [19].

II. Admittance Control

A. Modeling

This section discusses admittance control methods for one-degree-of-freedom systems. The model of a servo motor with a torque input τ_{m} (torque control mode) is described as

$$J_{\mathrm{m}}\ddot{q} = \tau_{\mathrm{m}} - \tau^{\mathrm{ext}} - \tau^{\mathrm{dis}}, \tag{1}$$

where J_{m}, $\ddot{q}$, τ^{ext}, and τ^{dis} denote the motor inertia, the acceleration response, the external torque, and the disturbance torque, respectively. The disturbance torque is the summation of all factors that interferes with motor drive except τ^{ext}. This paper assumes τ^{dis} as

$$\tau^{\mathrm{dis}} := \tau^{\mathrm{fri}} + \tau^{\mathrm{gra}} + \tau^{\mathrm{int}} + \tau^{\mathrm{par}}, \tag{2}$$

where τ^{fri}, τ^{gra}, τ^{int}, and τ^{par} are the friction torque, gravity effect, interference torque by other sources, and parameter fluctuation, respectively. The consideration is how to derive the torque input τ_{m} from the measurable response values and the estimable parameters. Note that this discussion holds for both the rotatory and the translational systems.

*This work was partially supported by JSPS KAKENHI Grant Number 21H04566 and Tateisi Science and Technology Foundation.

[1]Kosuke Shikata and Seiichiro Katsura are with the Department of System Design Engineering, Keio University, Yokohama 223-8522, Japan (e-mail: shikata@katsura.sd.keio.ac.jp; katsura@sd.keio.ac.jp).

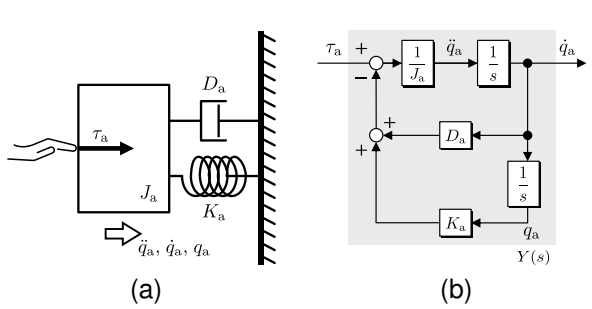

Fig. 1. Admittance causality. (a) Admittance model. (b) Block diagram.

B. Conventional Admittance Control

1) Admittance Causality: Admittance control determines motion: position q, velocity $\dot{q}$, and acceleration $\ddot{q}$, based on an applied torque. The transfer function from an applied torque τ_a to an output velocity $\dot{q}_\mathrm{a}$ describes an admittance causality.

$$\frac{\dot{q}_\mathrm{a}}{\tau_\mathrm{a}} = \frac{1}{J_\mathrm{a}s + D_\mathrm{a} + K_\mathrm{a}s^{-1}} =: Y(s), \tag{3}$$

where J_a, D_a, and K_a express the desired inertia, damping, and stiffness in the admittance causality, respectively. s is Laplace operator. Fig. 1(a) shows the admittance model when the causality holds. Fig. 1(b) signifies the block diagram of this causality. Since the diagram consists of the integrators and the desired parameters, the admittance controller sequentially derives the velocity reference that realizes the physical model shown in Fig. 1(a).

2) Conventional Structure: This explains the admittance controller that has been widely utilized. The admittance control aims to generate the velocity $\dot{q}$ and the position q have the admittance characteristics $Y(s)$ in response to the external torque τ^ext. The external torque, as well as disturbance torque τ^dis, is also a disturbance to the motor and must be suppressed. Fig. 2 shows the block diagram of the conventional control system. It has the inner velocity control loops to track the velocity reference of the admittance causality. Since the previous studies have generally adopted the velocity PI control, this paper also has that with the proportional gain K_p and the integral gain K_i. For the sake of simplicity, suppose that the sensor characteristic is $G_\mathrm{sen}(s) = 1$. Thereby, the transfer function from τ^ext to q and that from τ^dis to q are represented as

$$\frac{q}{\tau^\mathrm{ext}} = \frac{1}{s}\frac{(K_\mathrm{p}s + K_\mathrm{i})\,Y(s) - s}{J_\mathrm{m}s^2 + K_\mathrm{p}s + K_\mathrm{i}}, \tag{4}$$

$$\frac{q}{\tau^\mathrm{dis}} = -\frac{1}{J_\mathrm{m}s^2 + K_\mathrm{p}s + K_\mathrm{i}}, \tag{5}$$

respectively. Section II-D examines these transfer functions.

C. Proposed Admittance Control

This section explains the proposed admittance control based on DOB. The DOB obtains estimated disturbance from the torque input τ_m and the velocity response $\dot{q}$. The feedback of the estimated disturbance cancels the actual disturbance and realizes robust acceleration control.Moreover, the DOB

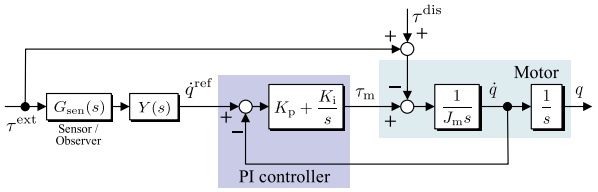

Fig. 2. Block diagram of conventional admittance control.

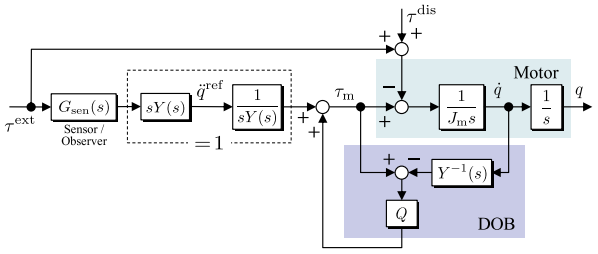

Fig. 3. Block diagram of the proposed admittance control.

considers a modeling error between the actual and the arbitrary nominal dynamics as a disturbance and attempts to compensate for them. Thus, this paper utilizes the compensation for the error between the actual admittance $1/J_\mathrm{m}s$ and the desired admittance $Y(s)$. Fig. 3 shows the block diagram of the proposed admittance control. The proposed controller incorporates the admittance as an inverse system in DOB. The designed parameter is only a Q-filter Q, and the Q-filter makes the transfer function proper. The proposed controller adopts a first-order low-pass filter, $Q = g/(s+g)$, due to the necessity of first-order derivatives on $Y^{-1}(s)$. g represents the cutoff frequency of the low-pass filter. The transfer function from τ^ext to q and that from τ^dis to q are described as

$$\frac{q}{\tau^\mathrm{ext}} = \frac{1}{g^{-1}J_\mathrm{m}s^3 + sY^{-1}(s)}, \tag{6}$$

$$\frac{q}{\tau^\mathrm{dis}} = -\frac{g^{-1}}{g^{-1}J_\mathrm{m}s^2 + Y^{-1}(s)}, \tag{7}$$

respectively. (6) and (7) are analyzed in the following section.

D. Comparisons

1) Frequency Responses: Fig. 4 compares the frequency responses of the proposed and the conventional admittance controls. The blue and red lines represent (4) and (6) responses, respectively. The motor inertia is set as $J_\mathrm{m} = 0.02$. For developing the desired admittance, the damping and the stiffness are fixed as $D_\mathrm{a} = 0.6$ and $K_\mathrm{f} = 2.4$. The inertia is given three varieties $J_\mathrm{a} = 0.1J_\mathrm{m}$, $J_\mathrm{a} = J_\mathrm{m}$, and $J_\mathrm{a} = 10J_\mathrm{m}$. Each of them is shown in Fig. 4(a), Fig. 4(b), and Fig. 4(c), respectively. The conventional controller utilizes the control parameters as $(K_\mathrm{i}, K_\mathrm{p}) = (60, 2), (120, 4), (180, 6)$. The cutoff in the proposed method is set as $g = 100,\ 200,\ 300$. The parameters of both controllers are determined so that each term of the characteristic equation is the same when J_a equals J_m. Each figure includes the correspondence between the increase in $(K_\mathrm{i}, K_\mathrm{p})$ or g and the response.

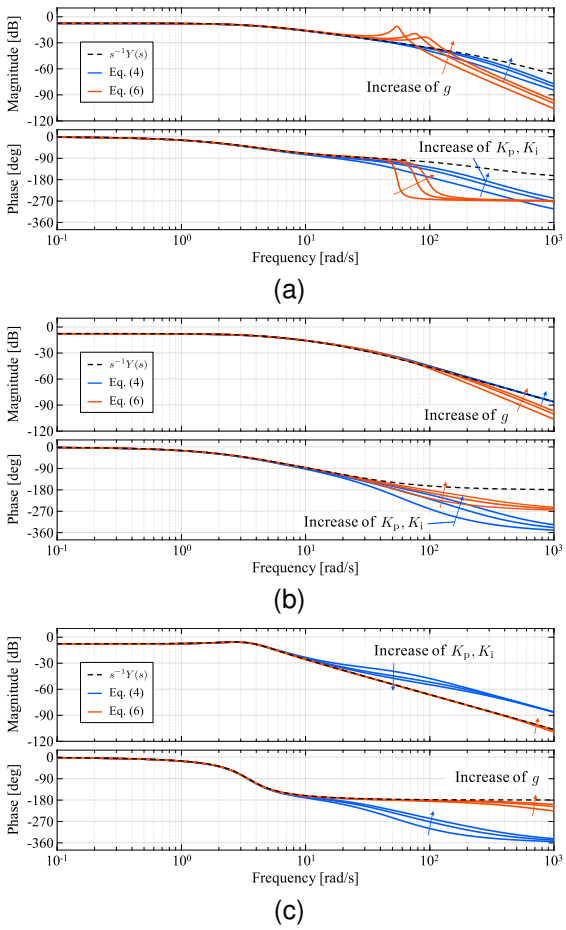

Fig. 4. Frequency responses of the proposed (red) and conventional (blue) admittance controls. (a) $J_\mathrm{a} = 0.1J_\mathrm{m}$. (b) $J_\mathrm{a} = J_\mathrm{m}$. (c) $J_\mathrm{a} = 10J_\mathrm{m}$.

Fig. 4 reveals that the proposed method matches the desired characteristic $s^{-1}Y(s)$ well when the desired inertia is larger than the motor inertia. The parameter g decides the frequency bandwidth where the proposed controller is valid. Equation (6) indicates that the relative influence of g depends on $J_\mathrm{m}Y(s)$. Thus, the bandwidth shifts according to $J_\mathrm{m}/J_\mathrm{a}$. The conventional controller has no similar effects, and the responses correspond the best when J_a equals J_m. Also, The responses of the conventional method have phase delay.

2) Steady-State Responses: For comparison of the steady-state disturbance suppression performances, the steady-state values of (5) and (7) are shown in (8) and (9), respectively.

- Steady-state of (5) in the conventional controller

$$\lim_{s\to 0} s\frac{q}{\tau^\mathrm{dis}}\frac{1}{s} = -\frac{1}{K_\mathrm{i}} \tag{8}$$

- Steady-state of (7) in the proposed controller

$$\lim_{s\to 0} s\frac{q}{\tau^\mathrm{dis}}\frac{1}{s} = -\lim_{s\to 0}\frac{Y(s)}{g} = 0 \tag{9}$$

Note that τ^dis is assumed to be a step disturbance. The conventional controller has a slight steady-state deviation, although the proposed one has no deviation. The conventional system requires an integral controller in the position dimension to suppress the deviation [11]. Because external torque is also applied to the motor as a disturbance, this deviation can degrade the admittance display.

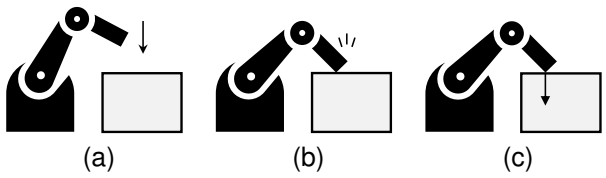

Fig. 5. Concept of transition in force control system. (a) Approach phase (b) Contact phase (c) Constrained phase.

III. Transitions in Force Control System

A. Robust Force Control

This section interprets robust force control based on the DOB-based admittance control. The torque input for the force control is determined as

$$\tau_\mathrm{m} = J_\mathrm{mn}K_\mathrm{f}(\tau^\mathrm{cmd} - \hat{\tau}^\mathrm{ext}) + \hat{\tau}^\mathrm{ext} + \hat{\tau}^\mathrm{dis}, \tag{10}$$

where K_f, τ^cmd, and $\hat{\tau}^\mathrm{ext}$ denote the force gain, the command torque, and the measured or estimated value of τ^ext, respectively. The second and third terms are compensation torque by DOB. If the compensation bandwidth is ideally large and $J_\mathrm{mn} = J_\mathrm{m}$ holds, the motion equation (1) turns into the following equation.

$$K_\mathrm{f}^{-1}\ddot{q} = \tau^\mathrm{cmd} - \hat{\tau}^\mathrm{ext} \tag{11}$$

Equation (11) expresses the system in which apparent inertia is K_f^{-1}. Moreover, if velocity feedback $-J_\mathrm{mn}K_\mathrm{v}\dot{q}$ to (10) is added, the motion equation is

$$K_\mathrm{f}^{-1}\ddot{q} + K_\mathrm{f}^{-1}K_\mathrm{v}\dot{q} = \tau^\mathrm{cmd} - \hat{\tau}^\mathrm{ext}, \tag{12}$$

where K_v represents the velocity feedback gain. Since DOB suppresses disturbances, the force control system is robust.

The proposed DOB-based admittance control is equivalent to (12). If g can be regarded as infinite, (6) turns into (13).

$$J_\mathrm{a}\ddot{q} + D_\mathrm{a}\dot{q} = \tau^\mathrm{cmd} - \hat{\tau}^\mathrm{ext}, \tag{13}$$

where the external torque is replaced by $\tau^\mathrm{cmd} - \hat{\tau}^\mathrm{ext}$ in this section. Accordingly, the desired admittance can be considered as the parameters of a robust force control system if K_a is zero. The proposed admittance control is the expansion of the robust force control, which gives us insights regarding the characteristics of physical motion and frequency limit in the force control system.

B. Transitions

Fig. 5 shows three phases of the force control system considered in this paper. Fig. 5(a) is an approach phase, which assumes that the manipulator has no contact with the environments and $\hat{\tau}^\mathrm{ext} = 0$. Fig. 5(b) represents a contact phase, which supposes a rapid switch from free motion to physical contact. In the contact phase, an impulsive force and vibratory response are problematic. Fig. 5(c) indicates a constrained phase in which force responses are stable after the contact phase. The constrained phase assumes that the manipulator performs some tasks on the surface at the desired force command.

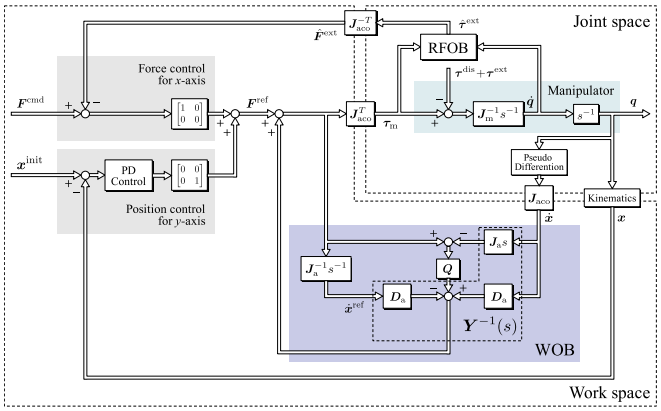

Fig. 6. Block diagram of the proposed force control utilizing the DOB-based admittance control.

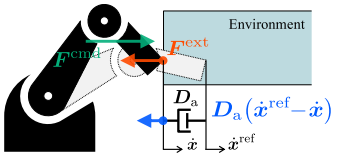

Fig. 7. Admittance model for safe contact regulation.

C. Safe Contact Regulation

Force control systems have mostly stayed the same in their structures even though they are under transitions of entirely different situations. This paper pays attention to the transitions between the three phases, especially from the approach phase to the contact phase. In the approach phase, the manipulator with the (11) controller moves at the constant acceleration since $\hat{\tau}^{\mathrm{ext}} = 0$. This acceleration contributes to the rapidity with which the task is initiated. Nevertheless, it also creates an excessive force during the transition to the contact phase. Making contact as softly as possible without losing this rapidity is required to perform a stable task. While the mechanical approaches provide stability against sudden contact, mechanical constraints on the contact direction and vibration generation during the approach phase are problems. This paper proposes a control method that supplies viscosity to the manipulator based on the proposed admittance control.

Fig. 6 shows the block diagram of the proposed force control system utilizing the DOB-based admittance control. $\boldsymbol{F}$ means the force matrix in workspace, and superscripts $^{\mathrm{cmd}}$, $^{\mathrm{ref}}$, $^{\mathrm{dis}}$, $^{\mathrm{ext}}$, and $^{\mathrm{init}}$ represent the command, the reference, the disturbance, the external, and the initial values, respectively. The DOB-based admittance control runs for achieving the desired admittance $Y(s)$. Fig. 6 has a workspace observer (WOB) [1], which is a DOB for workspace control. The proposed method is characterized by the design of the desired admittance. Fig. 7 represents the admittance model. In robust force control, the acceleration reference is realized as accelerated motion in the approach phase or surfaces as the force applied to the environments in the constrained phase. Therefore, acceleration reference is usually excessive in the contact phase, which is the instantaneous boundary between

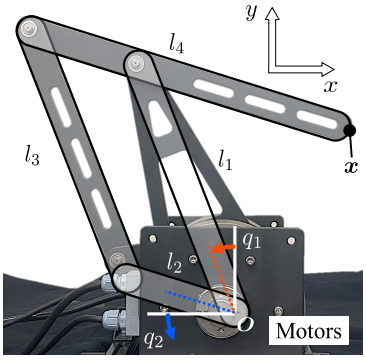

Fig. 8. Model of 2-DOF manipulator.

the approach and the constrained phases. The desired admittance of the proposed method attempts to suppress the excess acceleration reference as soon as possible. Because the acceleration reference is the output of the admittance (as shown in Fig.3), the velocity reference is also calculated based on the admittance. Meanwhile, the contact restricts the increase of the velocity response. Therefore, negative feedback of damping effect $\boldsymbol{D}_{\mathrm{a}}\left(\dot{\boldsymbol{x}}^{\mathrm{ref}} - \dot{\boldsymbol{x}}\right)$ suppresses the excess acceleration reference and decreases the external force during the contact phase. In the approach phase, the damping effect theoretically does not affect the accelerated motion because WOB/DOB achieves the robust acceleration control; $\ddot{\boldsymbol{x}}^{\mathrm{ref}} = \ddot{\boldsymbol{x}}$. When moving to the constrained phase, $\boldsymbol{D}_{\mathrm{a}} = \boldsymbol{0}$ makes the whole control system the same as the robust force control (11). Accordingly, the proposed force control realizes the contact regulation only with the gain-switching at the transition from the contact to the constrained phases. It induces no deceleration in the approach phase and requires no significant changes in control systems.

IV. Experiments

A. Setup

This section adopts the proposed method for a 2-DOF manipulator. Fig. 8 shows the model of the 2-DOF manipulator. $l_{\bigcirc}$ and $q_{\bigcirc}$ mean the length of each link and the angle of each motor. We confirmed that $l_1 = l_3 = 0.23$ m, $l_2 = 0.10$ m, and $l_4 = 0.30$ m. We defined the Cartesian coordinate $\boldsymbol{x} = [x, y]^T$ as shown in Fig. 8. The kinematics are derived as

$$\boldsymbol{x} = \begin{bmatrix} -l_1 \sin q_1 + (l_4 - l_2)\cos q_2 \\ l_1 \cos q_1 + (l_4 - l_2)\sin q_2 \end{bmatrix}. \tag{14}$$

The Jacobian matrix, which specifies $\dot{\boldsymbol{x}}$ for $\dot{\boldsymbol{q}}$, is shown as

$$\boldsymbol{J}_{\mathrm{aco}}(\boldsymbol{q}) = \begin{bmatrix} -l_1 \cos q_1 & -(l_4 - l_2)\sin q_2 \\ -l_1 \sin q_1 & +(l_4 - l_2)\cos q_2 \end{bmatrix}, \tag{15}$$

where $\boldsymbol{q} = [q_1, q_2]^T$ denotes the rotation angles of the motors. We designed the force controller in this 2-DOF system, considering the transition by the DOB-based admittance control. We applied the force control for the horizontal axis (x-axis) while utilizing the position control for the vertical axis (y-axis). External torque τ^{ext} was estimated by observers. WOB cancels the inter-axial disturbances [1].

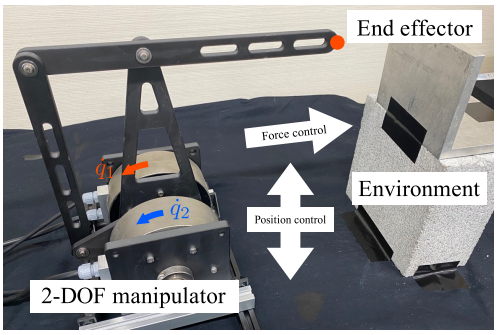

Fig. 9. Experimental setup.

TABLE I
EXPERIMENTAL PARAMETERS

Parameter	Value
$\boldsymbol{J}_{\mathrm{m}}$	$\mathrm{diag}(8.3\times10^{-3}\ \mathrm{kgm}^2,\ 3.4\times10^{-3}\ \mathrm{kgm}^2)$
g_{rfob}	140.0 rad/s
g_{diff}	500.0 rad/s
$\boldsymbol{Q}$	$\mathrm{diag}(60.0/(s{+}60.0),\ 0)$
$\boldsymbol{J}_{\mathrm{a}}$	$\mathrm{diag}(0.35\ \mathrm{kg},\ 0.20\ \mathrm{kg})$
$\boldsymbol{D}_{\mathrm{a}}$	$\mathrm{diag}(0.90\ \mathrm{Ns/m},\ 0.00\ \mathrm{Ns/m})$
$\boldsymbol{K}_{\mathrm{p}}$	$\mathrm{diag}(0.00\ \mathrm{N/m},\ 80.0\ \mathrm{N/m})$
$\boldsymbol{K}_{\mathrm{d}}$	$\mathrm{diag}(0.00\ \mathrm{Ns/m},\ 17.9\ \mathrm{Ns/m})$

Fig. 9 depicts the experimental environments. The manipulator was driven by two direct-drive motors (SGMCS-02BDC41; Yaskawa, Kitakyushu, Japan) with their amplifiers (SGD7S-2R1F00A; Yaskawa). We measured $\boldsymbol{q}$ using build-in encoders of the motors and calculated the angular velocity by pseudo-differentiation. The control period was 0.1 ms. The contact environments were a metallic object (Experiments 1) and a human hand (Experiments 2). Table I shows the experimental parameters and control parameters. The transition from contact to the constrained phase in the proposal was executed on a time-scheduled basis, and the time was set as 1.00 s and 3.00 s in Experiments 1 and 2, respectively. We incorporated the force control systems represented in (11) and (12) for comparison.

B. Results

1) Experiments 1: Fig. 10 shows the experimental results of Experiments 1. Fig. 10(a) is the overview in the x-axis and consists of upper force and lower position responses. Fig. 10(b) shows the enlarged view of the force responses in Fig. 10(a). Fig. 10(c) represents the position responses on the y-axis. We set the force command F_x^{cmd} as 1.5 N until 1.00 s and varied as represented by the black line in Figs. 10(a) and (b) after 1.00 s. The blue line indicates the conventional robust force control (11) with $\boldsymbol{K}_{\mathrm{f}} = \mathrm{diag}(2.86,\ 0.00)$. The manipulator contacted the environment at around 0.19 s. Fig. 10(b) shows that the response oscillated around F_x^{cmd} until about 0.50 s. After the oscillation was damped, the force response tracked the force command, which indicates that robust force control had good performance in the constrained phase. The green line depicts the responses of the other conventional method (12) with velocity feedback; $\boldsymbol{K}_{\mathrm{f}} = \mathrm{diag}(2.86,\ 0.00)$ and $\boldsymbol{K}_{\mathrm{v}} = \mathrm{diag}(28.6,\ 0.00)$.

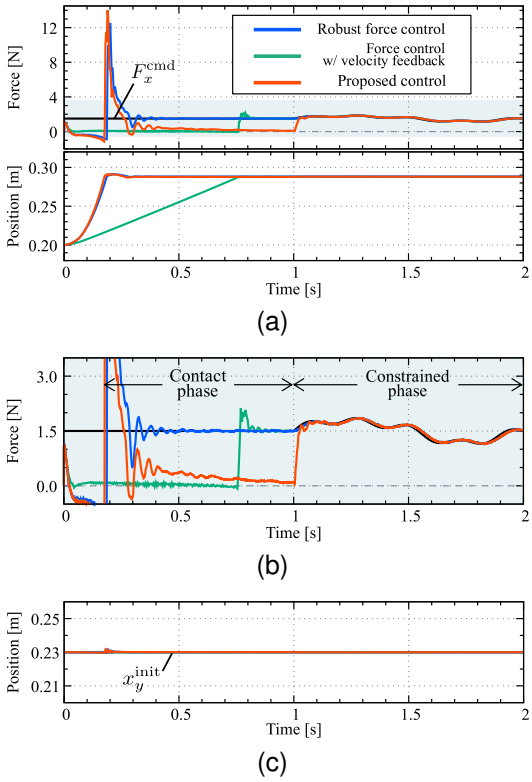

Fig. 10. Results of Experiments 1. (a) Overview of force control system (x-axis). Upper is force response, and lower is position response. (b) Enlarged view of the force response of (a). (c) Position response (y-axis).

The position response of Fig. 10(a) shows that the velocity feedback suppressed the accelerated motion in the approach phase. The force response implies that the magnitude of the impulsive force response depends on the velocity at the contact. The red line represents the proposed method. In the approach phase, it attained accelerated motion similar to the conventional robust force control (11). As shown in Figs. 10(a) and (b), the proposed control was under the contact phase from about 0.19 s to 1.00 s. During the contact phase, the damping effect by the admittance control suppressed the external force, which enabled to spend a period with transient oscillation while maintaining weak contact force. After $\boldsymbol{D}_{\mathrm{a}}$ was changed into $\boldsymbol{0}$, the proposed control achieved force tracking without overshooting. Moreover, we confirmed that all methods fulfilled the position control on the y-axis independently from the x-axis in Fig. 10(c) because of the WOB for canceling the inter-axial disturbances.

2) Experiments 2: Fig. 11 shows the experimental results of contacting and interacting with a human operator. In the approach phase, the operator received the end-effector of the moving manipulator. The controller independently regulated the y-axis position and the x-axis force. During the constrained phase, we gave the constant-amplitude, constant-cycle command to the y-axis position control. While Fig. 11(a) includes the responses of the conventional force control with velocity feedback, $\boldsymbol{K}_{\mathrm{v}} = \mathrm{diag}(5.71,\ 0.00)$, Fig. 11(b) represents the responses of the proposed method.

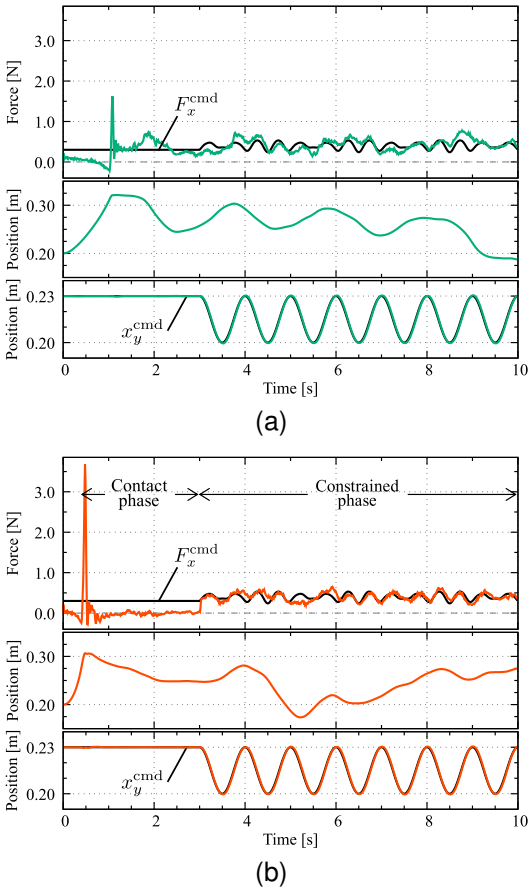

Fig. 11. Results of Experiments 2. (a) Force control with velocity feedback shown in (12). (b) Proposed control. Upper, middle, and lower are force response (x-axis), position response (x-axis), and position response (y-axis).

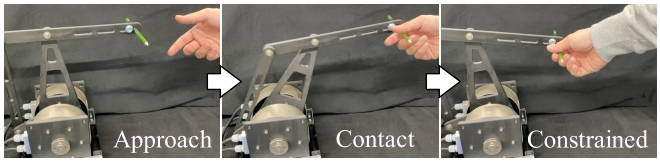

Fig. 12. Snapshots of Experiments 2.

Fig. 12 represents the snapshots while executing the proposed control. We set the force command F_x^{cmd} as 0.3 N until 3.00 s and varied as represented by the black line in Figs. 11.

Similarly to Experiments 1, the proposed method had the accelerated motion and damping effect, though the conventional method (12) did not have both. Although the accelerated motion led to the occurrence of the impulsive force, the force response is stable around 0 during the contact phase. The proposed control shifted smoothly to the robust force control with the beginning of the constrained phase.

V. Conclusion

This paper proposes the DOB-based admittance control and applies it to a force control system considering the phase transitions and suitable settings of admittance parameters. The proposed admittance control does not explicitly rely on the inner position or velocity control loop. The desired admittance shown in Fig.7 achieves safe contact regulation, considering the transitions between the three phases of force control. The proposed method is expected for applications such as robotic reproductions of artistic activities or skilled processing operations thanks to its environmental adaptation.

References

[1] N. Oda, T. Murakami, and K. Ohnishi, "A robust control strategy of redundant manipulator by workspace observer," *IEEJ Transactions on Industry Applications*, vol. 115, no. 8, pp. 991–998, 1995.

[2] K. Ohnishi, M. Shibata, and T. Murakami, "Motion control for advanced mechatronics," *IEEE/ASME Transactions on Mechatronics*, vol. 1, no. 1, pp. 56–67, 1996.

[3] E. Sariyildiz and K. Ohnishi, "On the explicit robust force control via disturbance observer," *IEEE Transactions on Industrial Electronics*, vol. 62, no. 3, pp. 1581–1589, 2015.

[4] A. Calanca and P. Fiorini, "Understanding environment-adaptive force control of series elastic actuators," *IEEE/ASME Transactions on Mechatronics*, vol. 23, no. 1, pp. 413–423, 2018.

[5] W. F. Rampeltshammer, A. Q. Keemink, and H. Van Der Kooij, "An improved force controller with low and passive apparent impedance for series elastic actuators," *IEEE/ASME transactions on mechatronics*, vol. 25, no. 3, pp. 1220–1230, 2020.

[6] H. Lee and S. Oh, "Series elastic actuators-driven parallel robot with wide-range impedance realization for balance assessment and training," *IEEE/ASME Transactions on Mechatronics*, vol. 27, no. 6, pp. 4619–4630, 2022.

[7] I. Payo, V. Feliu, and O. D. Cortázar, "Force control of a very lightweight single-link flexible arm based on coupling torque feedback," *Mechatronics*, vol. 19, no. 3, pp. 334–347, 2009.

[8] K. Shikata and S. Katsura, "Modal space control of bilateral system with elasticity for stable contact motion," *IEEJ Journal of Industry Applications*, vol. 12, no. 2, 2023.

[9] N. Motoi, T. Shimono, R. Kubo, and A. Kawamura, "Task realization by a force-based variable compliance controller for flexible motion control systems," *IEEE Transactions on Industrial Electronics*, vol. 61, no. 2, pp. 1009–1021, 2014.

[10] K. Haninger and M. Tomizuka, "Robust passivity and passivity relaxation for impedance control of flexible-joint robots with inner-loop torque control," *IEEE/ASME Transactions on Mechatronics*, vol. 23, no. 6, pp. 2671–2680, 2018.

[11] R. Kikuuwe, "A sliding-mode-like position controller for admittance control with bounded actuator force," *IEEE/ASME Transactions on Mechatronics*, vol. 19, no. 5, pp. 1489–1500, 2014.

[12] W. Zou, X. Chen, S. Li, P. Duan, N. Yu, and L. Shi, "Robust admittance control for human arm strength augmentation with guaranteed passivity: A complementary design," *IEEE/ASME Transactions on Mechatronics*, vol. 27, no. 6, pp. 5936–5947, 2022.

[13] M. Mujica, M. Crespo, M. Benoussaad, S. Junco, and J.-Y. Fourquet, "Robust variable admittance control for human–robot co-manipulation of objects with unknown load," *Robotics and Computer-Integrated Manufacturing*, vol. 79, p. 102408, 2023.

[14] A. Q. Keemink, H. van der Kooij, and A. H. Stienen, "Admittance control for physical human–robot interaction," *The International Journal of Robotics Research*, vol. 37, no. 11, pp. 1421–1444, 2018.

[15] M. J. Kim, W. Lee, J. Y. Choi, G. Chung, K.-L. Han, I. S. Choi, C. Ott, and W. K. Chung, "A passivity-based nonlinear admittance control with application to powered upper-limb control under unknown environmental interactions," *IEEE/ASME Transactions on Mechatronics*, vol. 24, no. 4, pp. 1473–1484, 2019.

[16] K. Samuel, K. Haninger, and S. Oh, "High-performance admittance control of an industrial robot via disturbance observer," in *IECON 2022 – 48th Annual Conference of the IEEE Industrial Electronics Society*, 2022, pp. 1–6.

[17] Y. Wu, T.-J. Tarn, and N. Xi, "Force and transition control with environmental uncertainties," in *Proceedings of 1995 IEEE International Conference on Robotics and Automation*, vol. 1, 1995, pp. 899–904.

[18] T.-J. Tarn, Y. Wu, N. Xi, and A. Isidori, "Force regulation and contact transition control," *IEEE Control Systems Magazine*, vol. 16, no. 1, pp. 32–40, 1996.

[19] P. Akella, V. Parra-Vega, S. Arimoto, and K. Tanie, "Discontinuous model-based adaptive control for robots executing free and constrained tasks," in *Proceedings of the 1994 IEEE International Conference on Robotics and Automation*, 1994, pp. 3000–3007 vol.4.